# Diffusion imaging markers of accelerated aging of the lower cingulum in subjective cognitive decline

Ryn Flaherty[1,2]*, Yu Veronica Sui[1], Arjun V. Masurkar[3,4], Rebecca A. Betensky[5], Henry Rusinek[1,6] and Mariana Lazar[1]

[1]Center for Advanced Imaging Innovation and Research, Department of Radiology, New York University Grossman School of Medicine, New York, NY, United States, [2]Vilcek Institute of Graduate Biomedical Sciences, New York University Grossman School of Medicine, New York, NY, United States, [3]Department of Neurology, New York University Grossman School of Medicine, New York, NY, United States, [4]Neuroscience Institute, New York University Grossman School of Medicine, New York, NY, United States, [5]Department of Biostatistics, New York University School of Global Public Health, New York, NY, United States, [6]Department of Psychiatry, New York University Grossman School of Medicine, New York, NY, United States

**Introduction:** Alzheimer's Disease (AD) typically starts in the medial temporal lobe, then develops into a neurodegenerative cascade which spreads to other brain regions. People with subjective cognitive decline (SCD) are more likely to develop dementia, especially in the presence of amyloid pathology. Thus, we were interested in the white matter microstructure of the medial temporal lobe in SCD, specifically the lower cingulum bundle that leads into the hippocampus. Diffusion tensor imaging (DTI) has been shown to differentiate SCD participants who will progress to mild cognitive impairment from those who will not. However, the biology underlying these DTI metrics is unclear, and results in the medial temporal lobe have been inconsistent.

**Methods:** To better characterize the microstructure of this region, we applied DTI to cognitively normal participants in the Cam-CAN database over the age of 55 with cognitive testing and diffusion MRI available ($N = 325$, 127 SCD). Diffusion MRI was processed to generate regional and voxel-wise diffusion tensor values in bilateral lower cingulum white matter, while T1-weighted MRI was processed to generate regional volume and cortical thickness in the medial temporal lobe white matter, entorhinal cortex, temporal pole, and hippocampus.

**Results:** SCD participants had thinner cortex in bilateral entorhinal cortex and right temporal pole. No between-group differences were noted for any of the microstructural metrics of the lower cingulum. However, correlations with delayed story recall were significant for all diffusion microstructure metrics in the right lower cingulum in SCD, but not in controls, with a significant interaction effect. Additionally, the SCD group showed an accelerated aging effect in bilateral lower cingulum with MD, AxD, and RD.

**Discussion:** The diffusion profiles observed in both interaction effects are suggestive of a mixed neuroinflammatory and neurodegenerative pathology. Left entorhinal cortical thinning correlated with decreased FA and increased RD, suggestive of demyelination. However, right entorhinal cortical thinning also correlated with increased AxD, suggestive of a mixed pathology. This may reflect combined pathologies implicated in early AD. DTI was more sensitive than cortical thickness to the associations between SCD, memory, and age. The combined effects of mixed pathology may increase the sensitivity of DTI metrics to variations with age and cognition.

# 1 Introduction

Early detection and treatment of Alzheimer's Disease (AD) is paramount in the prevention of neuronal degeneration and dementia. AD and related dementias were the 7th leading cause of death worldwide in 2019, affecting 55.2 million people (1). As of 2021, disability adjusted life years caused by AD are expected to more than triple by 2050 if current trends continue, with a particularly high impact forecasted in low and middle income countries (2). AD is characterized by a long preclinical stage noted by the deposition of amyloid plaques and tau tangles, followed by a destructive cascade of neurodegeneration leading to mild cognitive impairment and progression to dementia (3, 4). This cascade typically begins in the medial temporal lobe (5), a region important for memory (6). Early screening provides the patient an opportunity for future planning and lifestyle interventions to delay onset (3, 7–9). Therapeutic intervention in the preclinic stage also may interrupt the disease process before the onset of the neurodegeneration cascade (10). As disease modifying medications that disrupt this cascade such as aducanumab and lecanemab (11–13) become commercially available, early detection becomes increasingly important.

A promising avenue for early detection of AD is the study of subjective cognitive decline (SCD). SCD describes patients who complain of reduced memory performance or other cognitive decline but score normally on cognitive testing (14, 15). In cognitively unimpaired individuals above the age of 60, the prevalence of SCD is around 25% (16). Both multicenter studies and meta-analyses show increased rates of conversion to dementia in participants with SCD (14, 17, 18), with one meta-analysis showing SCD patients were twice as likely to develop dementia (14). In cognitively normal patients with positive amyloid and tau biomarkers, those with SCD are five times more likely to progress to mild cognitive impairment or dementia than those without cognitive complaints (19). SCD is also a better predictor of amyloid pathology than standard cognitive measures (20).

Despite its promise as a risk factor for dementia, SCD remains poorly understood. As AD is associated with atrophy of gray matter structures in the temporal, parietal, and cingulate cortices (21–23), many previous studies in SCD have focused on characterizing volume and cortical thickness of these regions (24–30), with inconsistent results (31–33). Prior research has also examined microstructural alterations in SCD using diffusion tensor imaging (DTI). DTI provides several diffusivity metrics, including fractional anisotropy (FA), axial (AxD), radial (RD), and mean (MD) diffusivity, which are all differentially affected by pathology. In a 2–3 year longitudinal study, DTI was shown to differentiate SCD patients who will progress to mild cognitive impairment from those who will not (34). Patients that converted to mild cognitive impairment also showed reduced cortical thickness and volume in the medial temporal lobe (34). However, DTI results in the medial temporal lobe have been inconsistent (35–37), potentially due, at least in part, to the relatively small samples used by some of the previous studies.

Therefore, the primary goal of this study was to further examine microstructural white matter changes in the medial temporal lobe using DTI, including associations with age and memory function, in SCD and unaffected control participants from Cambridge Center for Ageing and Neuroscience (Cam-CAN) (38, 39). Cam-CAN offers a large database of high quality anatomical, diffusion, fMRI, and magnetization transfer images alongside detailed behavioral, cognitive, and demographic measures. One other study reported on the incidence of SCD in Cam-CAN (40), and another showed increased MD and reduced FA with age across the white matter (41). However, to our knowledge this is the first study to study the relationship of SCD to diffusion imaging, cortical thickness, or volumes for brain structures other than hippocampus in the Cam-CAN dataset.

We chose to focus on the lower cingulum, or the white matter bundle leading to the hippocampus, as a region of interest (ROI) because as part of the medial temporal lobe, it is one of the most common starting points for neurodegeneration and tau pathology in AD (4). It is also an important region for memory (42). Further, the axons of the lower cingulum project to nearby gray matter regions that are vulnerable to neurodegeneration early in AD, including the entorhinal cortex, parahippocampal cortex, and the hippocampus (43).

A secondary goal of this work was to test whether cingulum microstructural variations relate to brain atrophy. Changes in brain structure volume and cortical thickness in SCD versus controls were examined for the lower cingulum and several AD signature gray matter regions including the hippocampus, parahippocampal cortex, entorhinal cortex, and temporal pole. Macrostructural metrics in areas associated with significant group differences were used as proxies for atrophy to examine the association of cingulum microstructure with neurodegeneration.

Using the large number of high-quality scans of older adults with SCD available from Cam-CAN, we may be able to detect microstructural changes not normally visible in smaller cohorts, lending new insights into the biology underlying SCD.

# 2 Materials and methods

## 2.1 Participant interview and cognitive testing

This study utilized the Cam-CAN dataset from the University of Cambridge, available at https://cam-can.mrc-cbu.cam.ac.uk/ (38, 39). Participants underwent a comprehensive cognitive battery and medical history examination to screen for neurological or psychiatric disorders. More details on data collection can be found in (39). Of the 3,000 Cam-CAN participants (38), we focused on those over the age of 55 with both cognitive health and diffusion MRI data available for a final N of 325. Of these participants, 127 answered affirmatively to the question "Do you feel you have any problems with your memory?"

These 127 participants were labeled as having subjective cognitive decline (SCD). The remaining 198 were used as control participants without SCD. Sex was determined by self-report. The Mini-Mental State Exam (MMSE) (44) was given as part of the home interview. Participants with an MMSE score lower than 24 or who failed to complete the MMSE were excluded (39). One control participant was missing MMSE scores in the dataset but was included in the analysis due to normal scores on all other tests and inclusion in the imaging cohort. Memory performance was assessed using story recall from WMS-III (45) during the home interview. Participants who passed screening had their memory tested in the clinic with an emotional memory (EM) task and a visual short-term memory (VSTM) task (39).

## 2.2 Magnetic resonance imaging acquisition and processing

The Cam-CAN MRI data was collected on a 3 T Siemens TIM Trio scanner with a 32-channel head coil. Diffusion weighted images included b values of 1,000 and 2000 s/mm$^2$ with 30 gradient directions each (39). Three images with $b = 0$ were also collected for each participant. Image noise and Gibbs ringing were attenuated using MRtrix version 3 (RRID:SCR_006971) tools dwidenoise (46–48) and mrdegibbs (49, 50). Motion correction was achieved using FSL version 6.0.4 (RRID:SCR_002823) tool mcflirt (51). The FSL DTIFIT algorithm was used to fit the diffusion tensor model with standard linear regression to each voxel, as well as to generate FA, MD, RD, and AxD maps for each participant (52). All images then underwent nonlinear transforms to standard space using FSL's Tract-Based Spatial Statistic (TBSS) pipeline (53). Rather than a skeleton mask, the lower right and left cingulum bundles were extracted from the ICBM-DTI-81 white-matter labels atlas (54) and employed as regions of interest (ROIs). The skeleton masks output by TBSS were not used in this analysis. Regional white matter volume of the cingulum bundle, cortical volume, and thickness of several grey matter regions were generated with FreeSurfer version 7 (RRID:SCR_001847) tools recon-all-clinical and synthseg (55), then visually quality controlled. Cortical structure ROIs analyzed were regions known to be susceptible to cortical thinning early in the Alzheimer's Disease course and included parahippocampal, entorhinal and temporal pole cortical thickness, as well as hippocampus and lower cingulum volume (21, 23). Brain structure volumes were divided by the intracranial volume to account for individual differences in head size.

TABLE 1 Demographic characteristics of the control and subjective cognitive decline (SCD) groups.

| | SCD (N = 128) | Control (N = 199) | Total (N = 327) | Test statistic | p value |
|---|---|---|---|---|---|
| *Sex* | | | | $\chi^2 = 0.238$ | 0.625 |
| FEMALE | 64 (50.0%) | 94 (47.2%) | 158 (48.3%) | | |
| MALE | 64 (50.0%) | 105 (52.8%) | 169 (51.7%) | | |
| *Age* | | | | $t = 1.04$ | 0.299 |
| Mean (SD) | 71.481 (8.941) | 70.424 (9.011) | 70.837 (8.985) | | |
| Range | 55.250–87.670 | 55.170–88.920 | 55.170–88.920 | | |
| *Income* | | | | $\chi^2 = 1.26$ | 0.939 |
| Less than £18,000 | 29 (22.7%) | 50 (25.1%) | 79 (24.2%) | | |
| £18,000 to 30,999 | 40 (31.2%) | 55 (27.6%) | 95 (29.1%) | | |
| £31,000 to 51,999 | 29 (22.7%) | 43 (21.6%) | 72 (22.0%) | | |
| £52,000 to 100,000 | 20 (15.6%) | 31 (15.6%) | 51 (15.6%) | | |
| Greater than £100,000 | 5 (3.9%) | 12 (6.0%) | 17 (5.2%) | | |
| Prefer not to answer | 5 (3.9%) | 8 (4.0%) | 13 (4.0%) | | |
| *Ethnicity* | | | | | |
| White | 126 (98.4%) | 194 (97.5%) | 320 (97.9%) | | |
| Mixed | 0 (0.0%) | 1 (0.5%) | 1 (0.3%) | | |
| Asian or Asian British | 1 (0.8%) | 2 (1.0%) | 3 (0.9%) | | |
| Black or Black British | 0 (0.0%) | 1 (0.5%) | 1 (0.3%) | | |
| Chinese | 0 (0.0%) | 0 (0.0%) | 0 (0.0%) | | |
| Other | 0 (0.0%) | 1 (0.5%) | 1 (0.3%) | | |
| Do not know | 0 (0.0%) | 0 (0.0%) | 0 (0.0%) | | |
| No answer | 1 (0.8%) | 0 (0.0%) | 1 (0.3%) | | |
| *Years of Education* | | | | $t = -0.571$ | 0.568 |
| Mean (SD) | 19.410 (4.087) | 19.697 (4.902) | 19.584 (4.595) | | |
| Range | 14.000–33.000 | 2.000–52.000 | 2.000–52.000 | | |

There were no between-group differences in sex, age, income, or years of education.

## 2.3 Statistical analysis

Differences between the two groups in age, memory performance, gender distribution, brain structure volume, cortical structure thickness, and lower cingulum diffusion microstructure were assessed with $t$-tests and chi-squared tests in R version 4.2 (RRID:SCR_000432). Outliers in the diffusion metric bilateral regional averages, cortical thicknesses, and volumes were presumed to be the result of image processing or acquisition errors and were excluded using Tukey's method (56). Sensitivity analyses compared models evaluated with and without outliers. Averages of each measure for the left and right lower cingulum ROIs were generated in MATLAB R2023a (RRID:SCR_001622). We then fit the following linear regression models:

$$\text{Metric} = \beta_0 + \beta_1 * \text{storyRecall} + \beta_2 * \text{group} + \beta_3 * \text{storyRecall} * \text{group} \tag{1}$$

$$\text{Metric} = \beta_0 + \beta_1 * \text{age} + \beta_2 * \text{group} + \beta_3 * \text{age} * \text{group} \tag{2}$$

$$\text{Metric} = \beta_0 + \beta_1 * \text{age} + \beta_2 * \text{storyRecall} + \beta_3 * \text{age} * \text{storyRecall} \tag{3}$$

$$\text{diffMetric} = \beta_0 + \beta_1 * \text{atophyMetric} + \beta_2 * \text{group} + \beta_3 * \text{atrophyMetric} * \text{group} \tag{4}$$

TABLE 2  Between-group comparison in memory performance.

|  | SCD | Control | Total | Test statistic | $p$ value | Cohen's D |
|---|---|---|---|---|---|---|
| MMSE |  |  |  | $t = -1.12$ | 0.264 | −0.13 |
| $N$ | 128 | 198 & | 326 |  |  |  |
| Mean (SD) | 28.547 (1.362) | 28.717 (1.306) | 28.650 (1.329) |  |  |  |
| Range | 25–30 | 25–30 | 25–30 |  |  |  |
| Immediate Story Recall** |  |  |  | $t = -2.73$ | 0.007 | −0.33 |
| $N$ | 128 | 199 | 327 |  |  |  |
| Mean (SD) | 12.617 (4.542) | 13.894 (3.381) | 13.394 (3.920) |  |  |  |
| Range | 3–23 | 4–23 | 3–23 |  |  |  |
| Delayed Story Recall** |  |  |  | $t = -3.20$ | 0.002 | −0.38 |
| $N$ | 128 | 199 | 327 |  |  |  |
| Mean (SD) | 10.461 (4.673) | 12.040 (3.800) | 11.422 (4.228) |  |  |  |
| Range | 0–22 | 0–21 | 0–22 |  |  |  |

MMSE, Mini-Mental State Exam. **$p < 0.01$. & One control participant is missing MMSE scores. However, they scored normally on story recall and denied any memory problems. Thus, we opted to include them in the analysis.

TABLE 3  Mean cortical thickness for temporal regions of interest (in mm) for the control and subjective cognitive decline (SCD) groups.

|  | SCD ($N = 125$ &) | Control ($N = 197$ &) | Test statistic | $p$ value | Cohen's D |
|---|---|---|---|---|---|
| Left entorhinal * |  |  | $t = -2.41$ | 0.017 | −0.27 |
| Mean (SD) | 2.947 (0.191) | 3.001 (0.207) |  |  |  |
| Range | 2.544–3.400 | 2.463–3.493 |  |  |  |
| Right entorhinal ** |  |  | $t = -2.86$ | 0.005 | −0.32 |
| Mean (SD) | 3.060 (0.176) | 3.119 (0.191) |  |  |  |
| Range | 2.620–3.484 | 2.606–3.605 |  |  |  |
| Left temporal pole |  |  | $t = -0.527$ | 0.599 | −0.06 |
| Mean (SD) | 3.446 (0.178) | 3.456 (0.161) |  |  |  |
| Range | 3.014–3.878 | 3.035–3.850 |  |  |  |
| Right temporal pole * |  |  | $t = -2.23$ | 0.026 | −0.27 |
| Mean (SD) | 3.630 (0.197) | 3.679 (0.174) |  |  |  |
| Range | 3.191–4.161 | 3.213–4.126 |  |  |  |

Between-group comparisons indicate decreased cortical thickness in SCD in left and right entorhinal cortices and the right temporal pole. *$p < 0.05$ and **$p < 0.01$. & There were 327 participants over the age of 55 with anatomical T1w images available. Two control participants and three SCD participants were excluded from the cortical thickness and brain structure volume analyses due to segmentation errors, for a total of 322 segmentations as detailed in this table.

where *diffMetric* is the regional average of each metric from DTI, *atrophyMetric* is the regional average cortical thickness or brain structure volume, *Metric* includes both diffusion and atrophy metrics, *storyRecall* is performance on the delayed story recall task, and *group* denotes SCD status (SCD versus control). Models 1, 2, and 4 included the group as a variable. Model 3 was examined across groups. All four models were employed for each diffusion metric. As we were primarily interested in the diffusion metrics' associations with atrophy, only cortical thicknesses and brain structure volumes that were different between groups ($p < 0.05$ and Cohen's D > 0.25) were included in Model 4. The linear regression models were fit in R. $p$-values smaller than 0.05 were considered statistically significant. In addition, voxel-wise analyses with multiple comparisons correction of the diffusion metrics within the extent of the lower cingulum bundles were calculated with threshold-free cluster enhancement (TFCE) including family-wise error correction ([57]) using FSL's randomise ([58]) with the same four models. While the voxel-wise analysis is more sensitive and allows for more robust multiple comparisons correction, linear regressions of regional averages allow for better visualization of effect sizes, slope directions, and interaction effects. Age and story recall were mean centered across groups for use with FSL's randomise, as described in the FSL documentation.

The code used for image processing and statistical analysis is available at: https://github.com/rf2485/camcan_scd_dMRI_paper.

# 3 Results

## 3.1 Group differences between SCD and controls

128 SCD participants and 199 control participants had imaging available, for a total of 327. There were no statistically significant differences between groups in age or sex distribution (Table 1). Of the memory tests employed in this study, only story recall was statistically significant between groups (Table 2). SCD participants performed significantly worse than control participants on both immediate and delayed story recall. We only used the delayed story recall score in the rest of our statistical analyses as it had a larger Cohen's $d$ effect size (0.37) than Immediate Story Recall (0.33) and MMSE (0.13). Three SCD participants and two control participants were excluded from the cortical thickness and brain structure volume analyses due to segmentation errors, leaving 322 datasets available for further analyses. SCD participants had thinner cortex in bilateral entorhinal cortex and right temporal pole (Table 3).

TABLE 4 Regional diffusion metric mean values for the subjective cognitive decline (SCD) and control groups in the left and right lower cingulum.

| | SCD (N = 127) | Control (N = 198) | Test statistic | p value | Cohen's D |
|---|---|---|---|---|---|
| Left FA | | | $t = 0.217$ | 0.829 | −0.03 |
| Mean (SD) | 0.296 (0.032) | 0.295 (0.035) | | | |
| Range | 0.231–0.398 | 0.186–0.387 | | | |
| Left MD | | | $t = 1.13$ | 0.259 | 0.07 |
| Mean (SD) | 0.621 (0.048) | 0.625 (0.047) | | | |
| Range | 0.491–0.738 | 0.482–0.744 | | | |
| Left AxD | | | $t = 0.680$ | 0.497 | 0.09 |
| Mean (SD) | 0.821 (0.060) | 0.820 (0.059) | | | |
| Range | 0.646–0.945 | 0.648e–0.97 | | | |
| Left RD | | | $t = 0.974$ | 0.331 | 0.06 |
| Mean (SD) | 0.521 (0.047) | 0.523 (0.045) | | | |
| Range | 0.414–0.637 | 0.389–0.647 | | | |
| Right FA | | | $t = 1.59$ | 0.112 | 0.18 |
| Mean (SD) | 0.299 (0.037) | 0.306 (0.036) | | | |
| Range | 0.206–0.397 | 0.220–0.389 | | | |
| Right MD | | | $t = −0.647$ | 0.518 | −0.13 |
| Mean (SD) | 0.634 (0.051) | 0.634 (0.046) | | | |
| Range | 0.500–0.787 | 0.478e–0.730 | | | |
| Right AxD | | | $t = −0.304$ | 0.761 | −0.04 |
| Mean (SD) | 0.852 (0.060) | 0.849 (0.058) | | | |
| Range | 0.665–1.000 | 0.608–0.962 | | | |
| Right RD | | | $t = −1.28$ | 0.201 | −0.17 |
| Mean (SD) | 0.534 (0.051) | 0.534 (0.046) | | | |
| Range | 0.409–0.678 | 0. 407–0.633 | | | |

No significant between-group differences are noted for any of the metrics. Diffusivity values are reported with units of $10^{-3}$ mm²/s.

There were 3 outliers for left entorhinal cortex thickness, 2 outliers for right entorhinal cortex, and 5 outliers for the right temporal pole. The results were robust to the removal of outliers. There were no significant group differences in any other cortical thicknesses or brain structure volumes analyzed (Supplementary Tables S1, S2).

127 SCD participants and 198 control participants had diffusion weighted images available, for a total of 325. There were no significant group differences in any of the diffusion metrics examined (Table 4). The results were robust to the removal of outliers.

## 3.2 Correlations between imaging and memory performance

For the right lower cingulum, there was a significant interaction effect between group and memory performance for regional mean MD, and RD (Model 1). Post-hoc analyses revealed that positive correlations with delayed story recall were significant for regional averages of FA, MD, AxD, and RD in SCD, but not in controls (Figure 1). Voxel-wise analyses with multiple comparisons correction confirmed this finding, with the addition of significant interaction effects for FA in a subset of voxels (Figure 2). There were no statistically significant findings between diffusion and memory in the left lower cingulum (Supplementary Table S3), nor were there any significant findings between memory and cortical thickness of grey matter regions studied (Supplementary Table S4). All findings were robust to the removal of outliers.

## 3.3 Correlations between imaging and age

As the risk for dementia increases with age (59), we were interested in the impact age had on the relationship between microstructure and story recall. To increase statistical power, our models only have three covariates each, particularly given the correlation between memory performance and group, as well as between memory performance and age. Model 2 includes age but does not include memory performance while Model 3 includes age but does not include group. In Model 2, there was a significant interaction effect between age and group in MD and AxD in right lower cingulum, which was robust to the removal of
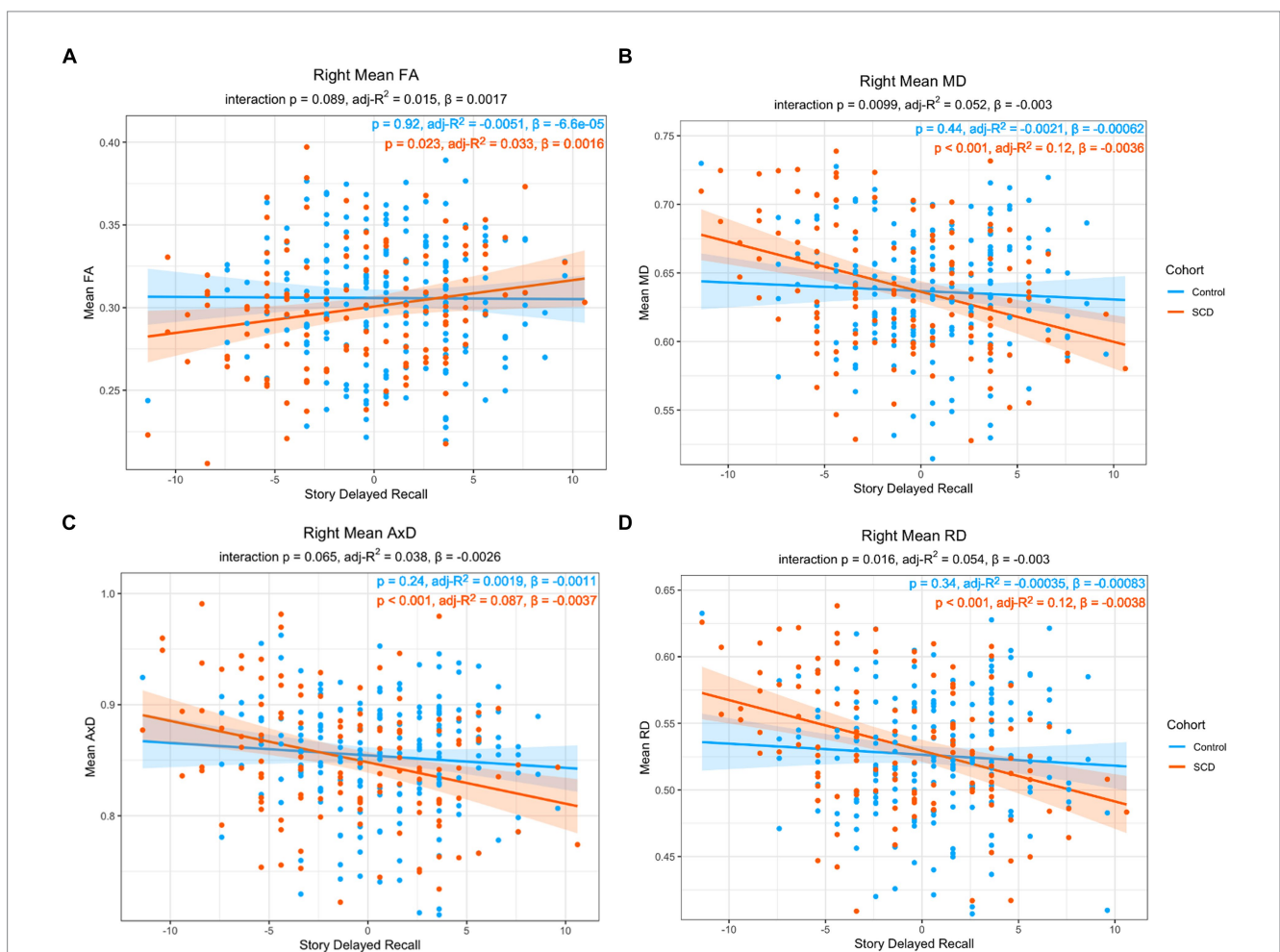


**FIGURE 1**
Linear regression of regional diffusion metric mean values in the whole right lower cingulum as a function of delayed story recall scores for **(A)** FA **(B)** MD **(C)** AxD and **(D)** RD. The p-values of the group by delayed story recall interaction are included in each chart subtitle. Interaction effects are significant for MD **(B)**, and RD **(D)**. The $p$-values of post-hoc within-group correlations between diffusion metrics and delayed story recall indicate a significant association between the diffusion metrics and memory function only in the SCD group in all diffusion metrics. Diffusivity values are reported with units of $10^{-3}$ mm$^2$/s.

outliers (Figure 3). Voxel-wise analyses with multiple comparisons correction confirmed this finding, with the addition of significant interaction effects for RD in a subset of voxels (Figure 4). A significant interaction effect for MD and AxD was also observed in the left lower cingulum after the removal of outliers. However, when outliers were included the $p$ value for MD increased from 0.005 to 0.078 and the p value for AxD increased from 0.003 to 0.025. All other findings were robust to the removal of outliers (Supplementary Table S5). In contrast, Model 3 did not show any significant interaction effects, indicating memory performance alone was not sensitive to the same group differences as SCD status despite the strong correlations between them (Supplementary Tables S6–S8). There were no significant interaction effects for cortical thickness in any of the regions studied (Supplementary Tables S8, S9). All findings were robust to the removal of outliers.

In post-hoc analyses, compared to controls, the SCD group showed a stronger correlation with age in MD, AxD, and RD, as well as a steeper slope, indicating an accelerated aging effect (Figure 3).

There was a significant main effect with age in all imaging metrics studied. Across both groups, FA decreased with age ($\beta = -0.00216$, $p < 0.001$), MD increased with age ($\beta = 2.51*10^{-4}$, $p < 0.001$), AxD increased with age ($\beta = 1.64*10^{-6}$, $p < 0.001$), and RD increased with age ($\beta = 3.06*10^{-6}$, $p < 0.001$). Left entorhinal ($\beta = -0.00654$, $p < 0.001$), right entorhinal ($\beta = 8.00*10^{-3}$, $p < 0.001$), and right temporal pole ($\beta = -0.00504$, $p < 0.001$) cortical thickness all decreased with age. All findings were robust to the removal of outliers.

## 3.4 Correlations between microstructure and cortical thickness

To further characterize the relationship between lower cingulum microstructure and atrophy, we modeled group differences in the relationship between each diffusion metric and cortical thickness of bilateral entorhinal cortex and right temporal pole using Model 4. The model was applied independently for the two hemispheres. There were
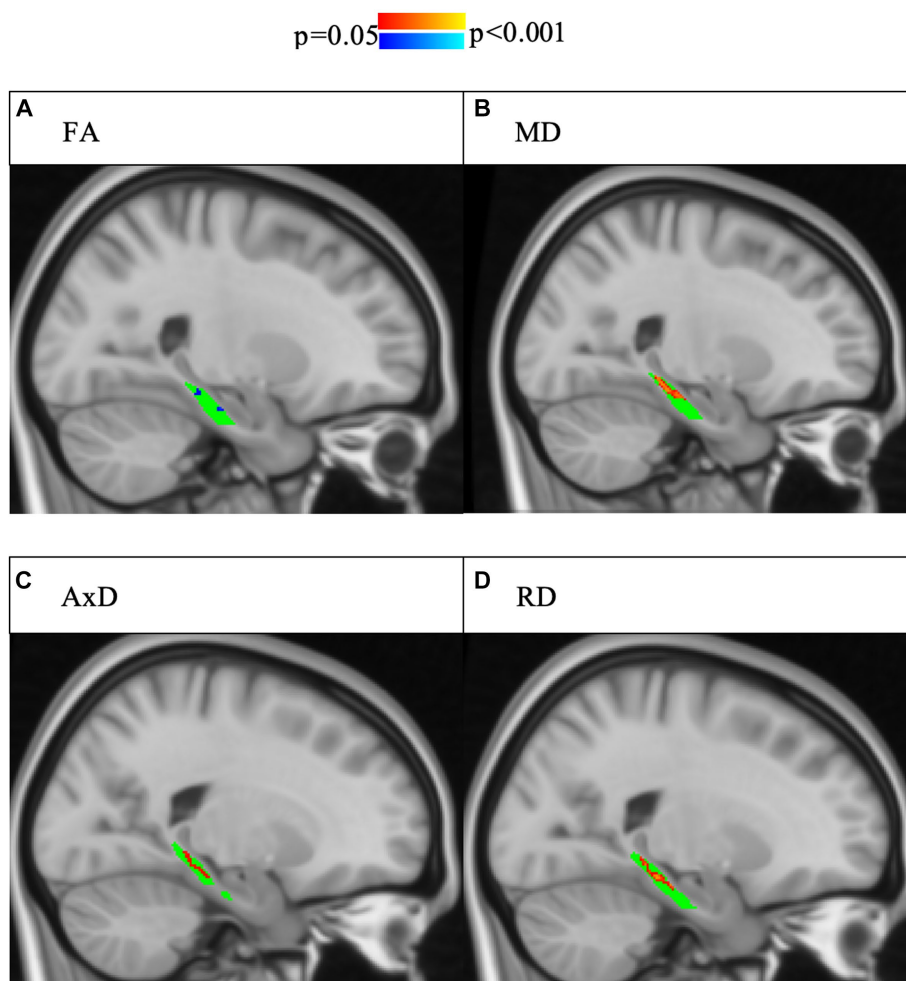


FIGURE 2
Interaction effects of cohort and delayed story recall score were confirmed by voxel-wise analysis with multiple comparisons correction of the whole right lower cingulum. Significant interactions ($p < 0.05$, corrected for multiple comparisons using threshold-free cluster enhancement) are highlighted, with blue indicating a more positive slope in SCD and red indicating a more negative slope in SCD. The region of interest (lower cingulum) is in green. Associations between increased memory scores and increased FA (A) as well as associations between decreased memory scores and increased (B) MD, (C) AD, and (D) RD were larger in SCD than controls.

no significant interaction effects between cortical thickness and group in any of the tests of Model 4 (Supplementary Tables S10–S12). However, there were significant main effects for diffusion microstructure across groups. Post-hoc analyses of diffusion microstructure by cortical thickness across groups revealed reduced cortical thicknesses in the left entorhinal, right entorhinal, and right temporal pole were all associated with decreased FA, increased MD, and increased RD (Figures 5–7). Additionally, reduced cortical thickness in right entorhinal cortex was associated with increased AxD (Figure 6). After adjusting for age, the associations between diffusion microstructure and cortical thickness were no longer significant (Supplementary Tables S13–S15).

## 4 Discussion

None of the cortical thickness measures showed any interaction between SCD status and age, SCD status and memory performance, or age and memory performance. Only diffusion metrics showed interaction effects between SCD status, memory, age, and neurobiological changes.

There was significant correlation between memory and all the diffusion markers examined (FA, MD, RD, and AxD) only in the SCD group. We found that decreased FA, increased MD, and increased RD had a stronger correlation with poor memory performance in SCD. This diffusion profile is typically associated with demyelination (60) or axonal loss (61, 62). However, both demyelination and axonal loss are associated with reduced AxD (63, 64). Here we see increased AxD, which has previously been observed in vasogenic edema associated with stroke (65), Monte Carlo simulations and tissue phantom models of vasogenic edema (66), and increased immunoreactivity associated with encephalitis (67, 68). Therefore, the diffusion profile noted here in SCD may indicate a mixed pathology of neurodegeneration and neuroinflammation. Our finding that cortical thickness and volume did not show any interaction between SCD status and memory performance further indicates that this diffusion profile is not explained by neurodegeneration alone. The effect sizes (adjusted $R^2$) of the associations between memory and diffusion metrics are small, but SCD and controls show different biological correlates with memory performance.
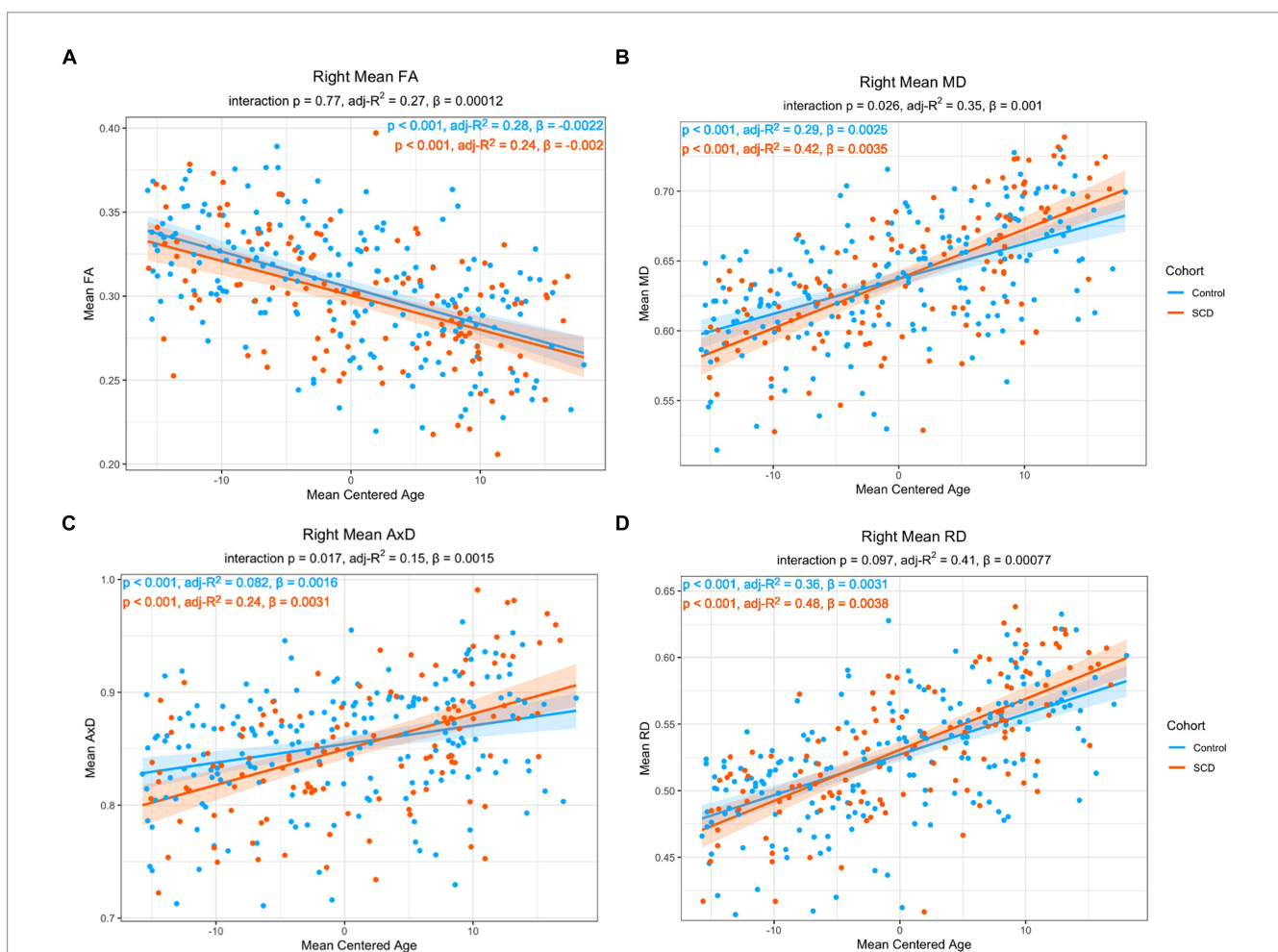


**FIGURE 3**
Linear regression of regional diffusion metric mean values in the whole right lower cingulum as a function of age for **(A)** FA **(B)** MD **(C)** AxD and **(D)** RD. The p-values of the group by age interaction are included in each chart subtitle. The interaction effects are significant for MD **(B)** and AxD **(C)** The adjusted R2 of post-hoc within-group correlations between diffusion metrics and age indicate a stronger association between the diffusion metrics and age in the SCD group in MD **(B)**, AxD **(C)**, and RD **(D)**. Diffusivity values are reported with units of $10^{-3}$ mm$^2$/s.
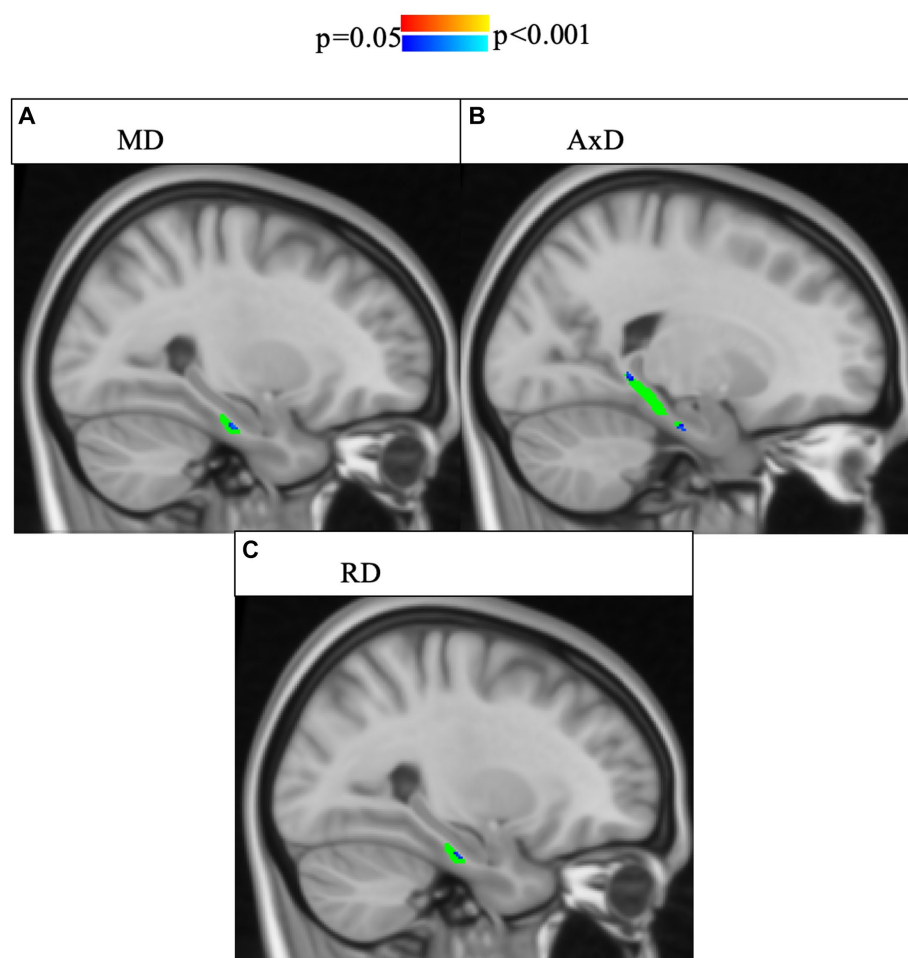
FIGURE 4
Interaction effects between cohort and age were confirmed by voxel-wise analysis with multiple comparisons correction of the whole right lower cingulum. Significant interactions ($p < 0.05$, corrected for multiple comparisons using threshold-free cluster enhancement) were found for areas of the right cingulum and are highlighted in blue shades. The region of interest (lower cingulum) is in green. Associations between increased age and increased **(A)** MD, **(B)** AxD, and **(C)** RD were stronger in SCD than in controls. FA is not pictured because no voxels showed a significant interaction effect.

When including age in our statistical modeling, participants with SCD present with an accelerated aging effect in diffusion microstructure, showing steeper variations with age. Similar to our findings in memory performance, this accelerated aging effect was noted for increased MD, RD, and AxD. As noted above, an increase in both RD and AxD is more suggestive of a mixed neurodegeneration and neuroinflammation pathology, rather than neurodegeneration alone (69–71). Cortical thickness did not capture this accelerated aging effect, further supporting that neurodegeneration alone was insufficient to explain these diffusion findings. The interaction between memory performance and age was not significant for any diffusion, cortical thickness, or cortical volume measures. Thus, SCD status was more sensitive than memory performance to differences in diffusion microstructure associated with aging.

Previous research investigating DTI in SCD has largely only included FA and MD in their analyses. Of these studies, some have reported no statistically significant findings in the lower cingulum (37, 72, 73). These mixed findings may reflect, in part, the presence of field inhomogeneities reducing the signal-to-noise ratio of the diffusion images in the lower cingulum (74), as many studies do report reduced FA and increased MD in SCD in bilateral cingulum (26, 29, 42) or increased MD in SCD in the left lower cingulum (75). These later data are comparable to our findings of increased MD and reduced FA in right lower cingulum with age and memory performance in SCD.

Studies that do include AxD and RD in their analyses also have mixed results, with some studies finding no changes in the lower cingulum (35, 36, 76). However, other studies found increased RD in bilateral lower cingulum (34, 77) and in left lower cingulum (78). While other studies have found increased AxD in SCD (79, 80), none of these have localized to the lower cingulum. In our results, we find increased RD and AxD in the right lower cingulum related to age and poor memory performance in SCD, with few significant results in the left. This contrasts with past studies that found increased RD and no changes in AxD in the left lower cingulum.

In mild cognitive impairment, increased RD and MD, but not AxD, were found to be associated with low cognitive performance (81, 82), representing a diffusion profile more suggestive of demyelination (83) and neurodegeneration (84). Prior research has shown a

nonmonotonic trajectory of diffusion metrics in early AD, suggestive of an early inflammatory process followed by a neurodegenerative process (69–71). This includes an increase in free water, MD, and neurite density during the "inflammatory" stage followed by a decrease during the "degeneration" stage (71). Thus, our findings in SCD may be capturing an earlier, more inflammatory timepoint in the AD course occurring in parallel with neurodegeneration and the deposition of protein aggregates.

While we found group differences in cortical thickness in bilateral entorhinal cortex and right temporal pole, the correlations between cortical thickness and diffusion microstructural metrics did not differ between groups. Both AD and aging-related neurodegeneration are typically greater on the left than on the right (85), but here we found group differences in cortical thinning in more regions on the right than on the left. Cortical thinning in our study was associated with decreased FA, increased RD, and increased MD in the left lower cingulum and right temporal pole, a profile suggestive of demyelination (83) and suggestive of diffusion microstructural changes related to aging (86). In the right hemisphere, we found that cortical thinning was associated with increased AxD in addition to decreased FA, increased MD, and increased RD, suggesting a more mixed pathology, albeit with a small effect size.

In summary, DTI appeared to be more sensitive than cortical thickness to the associations between SCD, memory, and age. DTI metrics are aggregate measures of water diffusivity across microstructural compartments (87) and may reflect combinations of pathologies implicated in early AD, including demyelination, neurodegeneration, protein aggregation, neurovascular abnormalities, disrupted connectivity, and inflammation (88, 89). Thus, the combined effects of mixed pathology may increase the sensitivity of the DTI metrics to microstructural variations with age and cognition.

Strengths of this study include the large number of subjective cognitive decline participants scanned on the same MRI machine, at the same location, with the same protocol. This allowed us to achieve better sensitivity in the diffusion metric analysis. The participants have a diversity of years of education and income brackets. They are also evenly distributed between genders. No statistically significant differences in demographics were observed between cohorts.

Limitations of this study include a lack of ethnic diversity in the cohort. There also is no longitudinal data, Alzheimer's biomarkers, or genetic data available from this dataset. Due to the lack of biomarker and longitudinal data in this study, it is difficult to interpret what pathologies underlie the changes observed in diffusion metrics here. Future work will apply similar analyses to a smaller dataset with
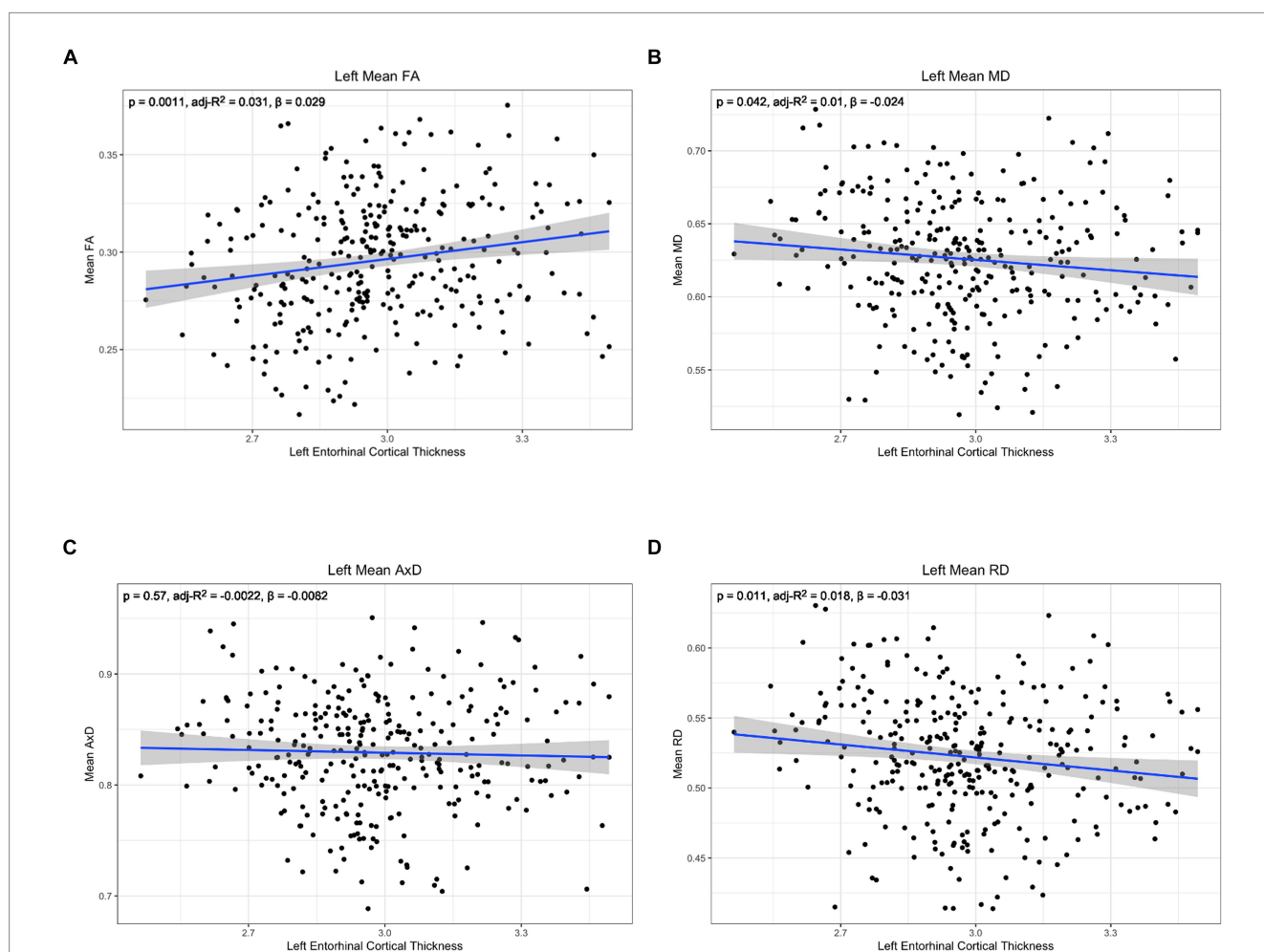


FIGURE 5
Correlation between diffusion metrics in the whole left lower cingulum and thickness of the left entorhinal cortex for (A) FA (B) MD (C) AxD and (D) RD. The correlation is significant for FA (A), MD (B), and RD (D). Diffusivity values are reported with units of $10^{-3}$ mm$^2$/s.

**FIGURE 6**
Correlation between diffusion metrics in the whole right lower cingulum and thickness of the right entorhinal cortex for **(A)** FA **(B)** MD **(C)** AxD and **(D)** RD. The correlation is significant for all diffusion metrics. Diffusivity values are reported with units of $10^{-3}$ mm$^2$/s.
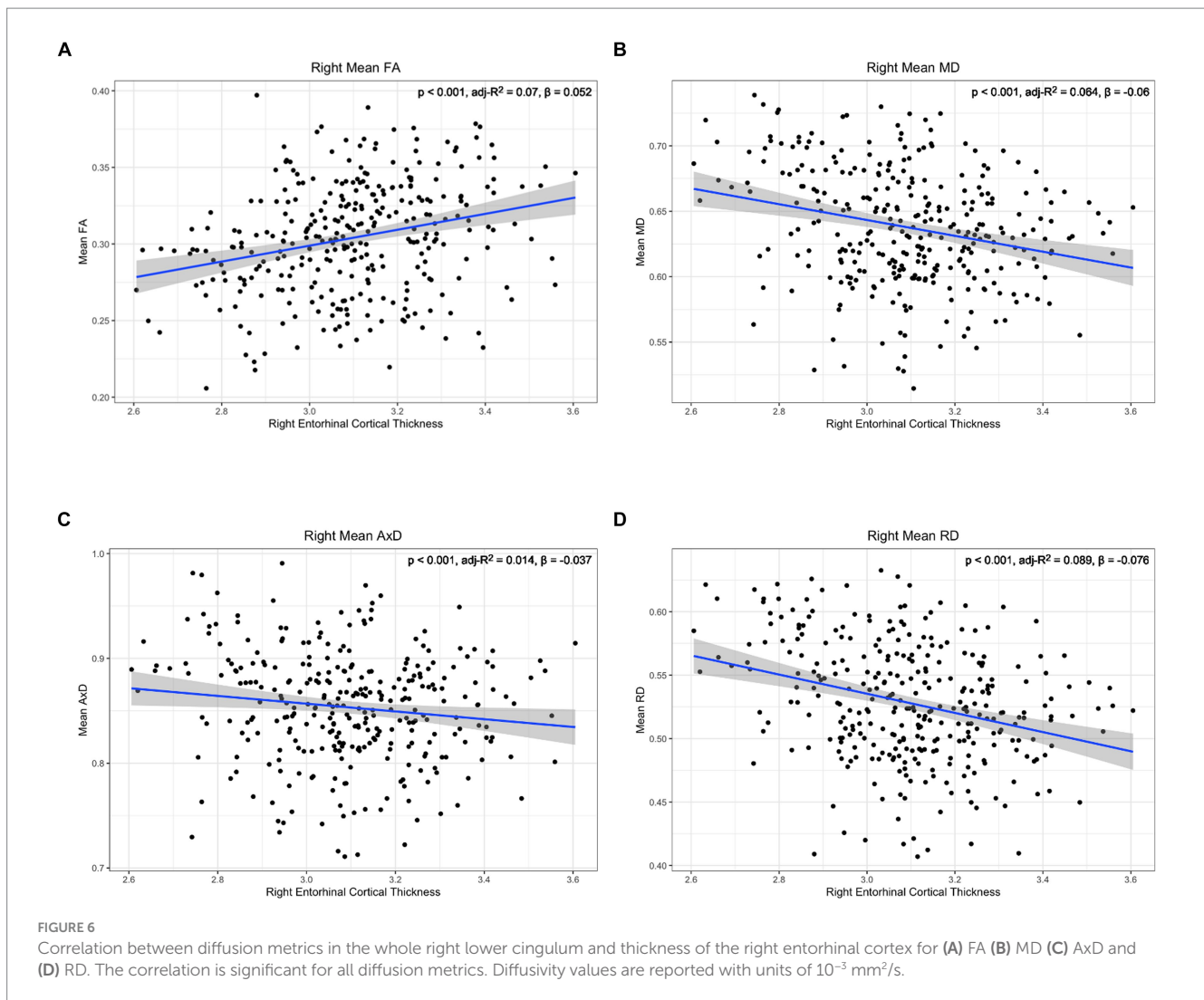
better biomarker data and longitudinal follow up. Magnetization transfer imaging data available from Cam-CAN may further clarify the MRI microstructure variations in this particular cohort.

## Data availability statement

The original contributions presented in the study are included in the article/Supplementary material, further inquiries can be directed to the corresponding author.
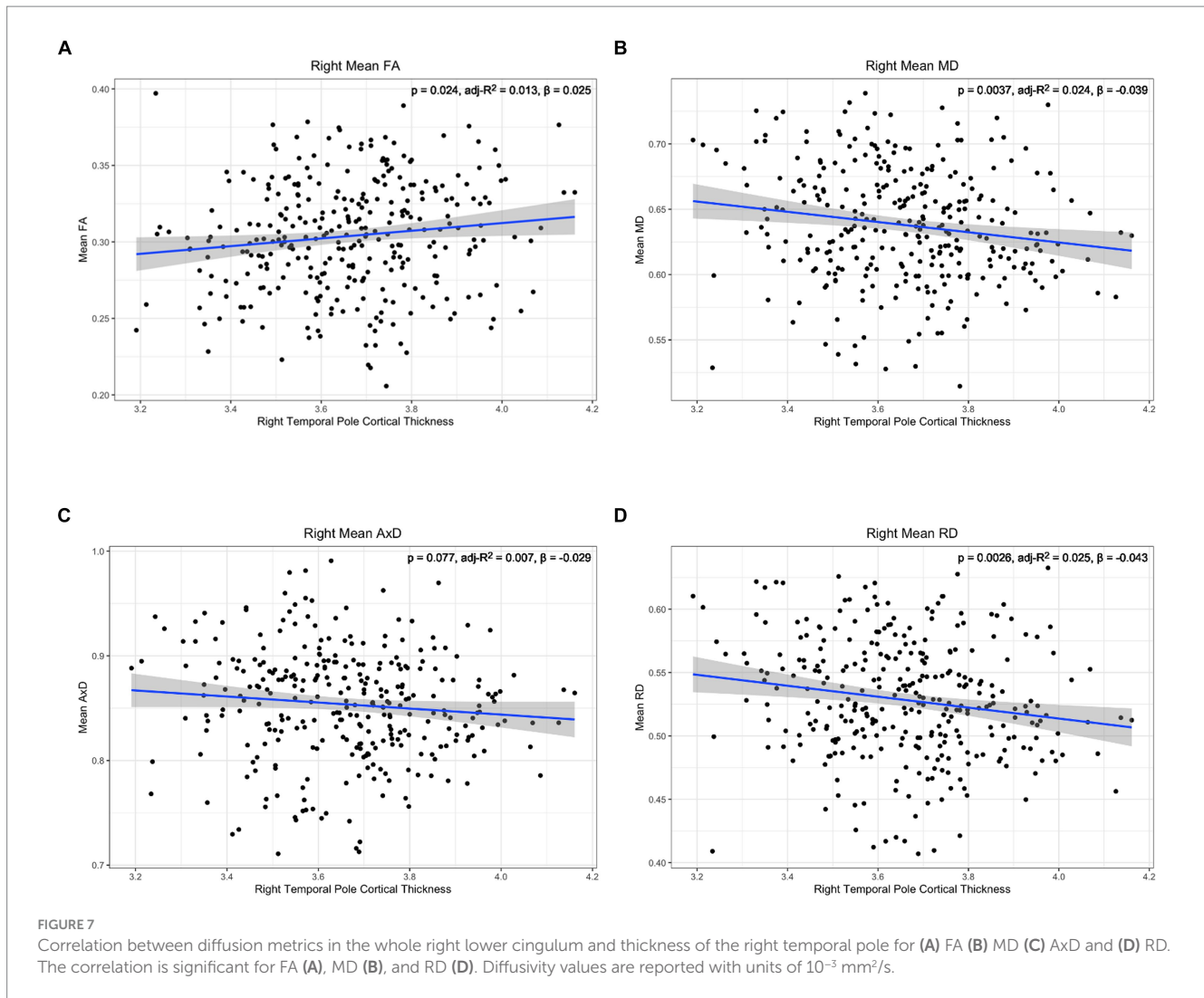
## Ethics statement

The studies involving humans were approved by Cambridgeshire 2 Research Ethics Committee (reference: 10/H0308/50). The studies were conducted in accordance with the local legislation and institutional requirements. The participants provided their written informed consent to participate in this study. Written informed consent was obtained from the individual(s) for the publication of any potentially identifiable images or data included in this article.

## Author contributions

RF: Formal analysis, Methodology, Visualization, Writing – original draft, Writing – review & editing. YS: Methodology, Writing – original draft, Writing – review & editing. AM: Supervision, Writing – original draft, Writing – review & editing. RB: Writing – review & editing, Formal analysis. HR: Supervision, Writing – original draft, Writing – review & editing. ML: Funding acquisition, Project administration, Supervision, Writing – original draft, Writing – review & editing.

## Funding

**FIGURE 7**
Correlation between diffusion metrics in the whole right lower cingulum and thickness of the right temporal pole for **(A)** FA **(B)** MD **(C)** AxD and **(D)** RD. The correlation is significant for FA **(A)**, MD **(B)**, and RD **(D)**. Diffusivity values are reported with units of $10^{-3}$ mm$^2$/s.

## Conflict of interest

The authors declare that the research was conducted in the absence of any commercial or financial relationships that could be construed as a potential conflict of interest.

## Publisher's note

All claims expressed in this article are solely those of the authors and do not necessarily represent those of their affiliated organizations, or those of the publisher, the editors and the reviewers. Any product that may be evaluated in this article, or claim that may be made by its manufacturer, is not guaranteed or endorsed by the publisher.

## Supplementary material

The Supplementary material for this article can be found online at: https://www.frontiersin.org/articles/10.3389/fneur.2024.1360273/full#supplementary-material

## References

1. Global Health estimates 2020: deaths by cause, age, sex, by country and by region, 2000–2019. World Health Organization, (2020)

2. Bloom D, Chen S, Counts N, Han R, Malik S, Nandi A, et al. Addressing Alzheimer's disease and related dementias to realise the promise of the UN's 'decade of healthy ageing'. *VoxEU*. (2021):26.

3. Porsteinsson AP, Isaacson RS, Knox S, Sabbagh MN, Rubino I. Diagnosis of early Alzheimer's disease: clinical practice in. *J Prev Alzheimers Dis*. (2021) 2021:1–16.

4. Jack CR, Knopman DS, Jagust WJ, Petersen RC, Weiner MW, Aisen PS, et al. Tracking pathophysiological processes in Alzheimer's disease: an updated hypothetical

model of dynamic biomarkers. *Lancet Neurol*. (2013) 12:207–16. doi: 10.1016/S1474-4422(12)70291-0

5. Frisoni GB, Boccardi M, Barkhof F, Blennow K, Cappa S, Chiotis K, et al. Strategic roadmap for an early diagnosis of Alzheimer's disease based on biomarkers. *Lancet Neurol*. (2017) 16:661–76. doi: 10.1016/S1474-4422(17)30159-X

6. Bannerman DM, Rawlins JN, McHugh SB, Deacon RM, Yee BK, Bast T, et al. Regional dissociations within the hippocampus—memory and anxiety. *Neurosci Biobehav Rev*. (2004) 28:273–83. doi: 10.1016/j.neubiorev.2004.03.004

7. de Levante RD. The knowledge and attitudes of primary care and the barriers to early detection and diagnosis of Alzheimer's disease. *Medicina*. (2022) 58:70906. doi: 10.3390/medicina58070906

8. The need for early detection and treatment in Alzheimer's disease. *EBioMedicine*. (2016) 9:1–2. doi: 10.1016/j.ebiom.2016.07.001

9. Ahmed H, Soliman H, Elmogy M. Early detection of Alzheimer's disease using single nucleotide polymorphisms analysis based on gradient boosting tree. *Comput Biol Med*. (2022) 146:105622. doi: 10.1016/j.compbiomed.2022.105622

10. Hyman BT. Amyloid-dependent and amyloid-independent stages of Alzheimer disease. *Arch Neurol*. (2011) 68:1062–4. doi: 10.1001/archneurol.2011.70

11. van Dyck CH, Swanson CJ, Aisen P, Bateman RJ, Chen C, Gee M, et al. Lecanemab in early Alzheimer's disease. *N Engl J Med*. (2023) 388:9–21. doi: 10.1056/NEJMoa2212948

12. Shi M, Chu F, Zhu F, Zhu J. Impact of anti-amyloid-beta monoclonal antibodies on the pathology and clinical profile of Alzheimer's disease: a focus on Aducanumab and Lecanemab. *Front Aging Neurosci*. (2022) 14:870517. doi: 10.3389/fnagi.2022.870517

13. Budd Haeberlein S, Aisen P, Barkhof F, Chalkias S, Chen T, Cohen S, et al. Two randomized phase 3 studies of aducanumab in early Alzheimer's disease. *J Prev Alzheimers Dis*. (2022) 30:1–14. doi: 10.14283/jpad.2022.30

14. Jessen F, Amariglio RE, Van Boxtel M, Breteler M, Ceccaldi M, Chételat G, et al. A conceptual framework for research on subjective cognitive decline in preclinical Alzheimer's disease. *Alzheimers Dement*. (2014) 10:844–52. doi: 10.1016/j.jalz.2014.01.001

15. Jessen F, Amariglio RE, Buckley RF, van der Flier WM, Han Y, Molinuevo JL, et al. The characterisation of subjective cognitive decline. *Lancet Neurol*. (2020) 19:271–8. doi: 10.1016/S1474-4422(19)30368-0

16. Rohr S, Pabst A, Riedel-Heller SG, Jessen F, Turana Y, Handajani YS, et al. Estimating prevalence of subjective cognitive decline in and across international cohort studies of aging: a COSMIC study. *Alzheimers Res Ther*. (2020) 12:167. doi: 10.1186/s13195-020-00734-y

17. Jonker C, Geerlings MI, Schmand B. Are memory complaints predictive for dementia? A review of clinical and population-based studies. *Int J Geriatr Psychiatry*. (2000) 15:983–91. doi: 10.1002/1099-1166(200011)15:11<983::AID-GPS238>3.0.CO;2-5

18. Slot RE, Sikkes SA, Berkhof J, Brodaty H, Buckley R, Cavedo E, et al. Subjective cognitive decline and rates of incident Alzheimer's disease and non-Alzheimer's disease dementia. *Alzheimers Dement*. (2019) 15:465–76. doi: 10.1016/j.jalz.2018.10.003

19. Buckley RF, Maruff P, Ames D, Bourgeat P, Martins RN, Masters CL, et al. Subjective memory decline predicts greater rates of clinical progression in preclinical Alzheimer's disease. *Alzheimers Dement*. (2016) 12:796–804. doi: 10.1016/j.jalz.2015.12.013

20. Amariglio RE, Becker JA, Carmasin J, Wadsworth LP, Lorius N, Sullivan C, et al. Subjective cognitive complaints and amyloid burden in cognitively normal older individuals. *Neuropsychologia*. (2012) 50:2880–6. doi: 10.1016/j.neuropsychologia.2012.08.011

21. Pettigrew C, Soldan A, Zhu Y, Wang MC, Moghekar A, Brown T, et al. Cortical thickness in relation to clinical symptom onset in preclinical AD. *NeuroImage Clin*. (2016) 12:116–22. doi: 10.1016/j.nicl.2016.06.010

22. Dincer A, Gordon BA, Hari-Raj A, Keefe SJ, Flores S, McKay NS, et al. Comparing cortical signatures of atrophy between late-onset and autosomal dominant Alzheimer disease. *NeuroImage Clin*. (2020) 28:102491. doi: 10.1016/j.nicl.2020.102491

23. Dickerson BC, Bakkour A, Salat DH, Feczko E, Pacheco J, Greve DN, et al. The cortical signature of Alzheimer's disease: regionally specific cortical thinning relates to symptom severity in very mild to mild AD dementia and is detectable in asymptomatic amyloid-positive individuals. *Cereb Cortex*. (2009) 19:497–510. doi: 10.1093/cercor/bhn113

24. Chen J, Wang S, Chen R, Liu Y. Editorial: Neuroimaging biomarkers and cognition in Alzheimer's disease Spectrum. *Front Aging Neurosci*. (2022) 14:848719. doi: 10.3389/fnagi.2022.848719

25. Dauphinot V, Bouteloup V, Mangin JF, Vellas B, Pasquier F, Blanc F, et al. Subjective cognitive and non-cognitive complaints and brain MRI biomarkers in the MEMENTO cohort. *Alzheimer's Dement: Diagn Assess Dis Monit*. (2020) 12:12051. doi: 10.1002/dad2.12051

26. Hong YJ, Yoon B, Shim YS, Ahn KJ, Yang DW, Lee J-H. Gray and white matter degenerations in subjective memory impairment: comparisons with normal controls and mild cognitive impairment. *J Korean Med Sci*. (2015) 30:1652–8. doi: 10.3346/jkms.2015.30.11.1652

27. Lista S, Molinuevo JL, Cavedo E, Rami L, Amouyel P, Teipel SJ, et al. Evolving evidence for the value of Neuroimaging methods and biological markers in subjects categorized with subjective cognitive decline. *J Alzheimers Dis*. (2015) 48:S171–91. doi: 10.3233/JAD-150202

28. Parker AF, Smart CM, Scarapicchia V, Gawryluk JR. For the Alzheimer's disease Neuroimaging I. Identification of earlier biomarkers for Alzheimer's disease: a multimodal Neuroimaging study of individuals with subjective cognitive decline. *J Alzheimers Dis*. (2020) 77:1067–76. doi: 10.3233/JAD-200299

29. Ryu SY, Lim EY, Na S, Shim YS, Cho JH, Yoon B, et al. Hippocampal and entorhinal structures in subjective memory impairment: a combined MRI volumetric and DTI study. *Int Psychogeriatr*. (2017) 29:785–92. doi: 10.1017/S1041610216002349

30. Wang X, Huang W, Su L, Xing Y, Jessen F, Sun Y, et al. Neuroimaging advances regarding subjective cognitive decline in preclinical Alzheimer's disease. *Mol Neurodegener*. (2020) 15:55. doi: 10.1186/s13024-020-00395-3

31. Morrison C, Dadar M, Shafiee N, Villeneuve S. Louis Collins D, for Alzheimer's disease Neuroimaging I. Regional brain atrophy and cognitive decline depend on definition of subjective cognitive decline. *NeuroImage Clin*. (2022) 33:102923. doi: 10.1016/j.nicl.2021.102923

32. Parker AF, Ohlhauser L, Scarapicchia V, Smart CM, Szoeke C, Gawryluk JR. A systematic review of neuroimaging studies comparing individuals with subjective cognitive decline to healthy controls. *J Alzheimers Dis*. (2022) 86:1545–67. doi: 10.3233/JAD-215249

33. Pini L, Wennberg AM. Structural imaging outcomes in subjective cognitive decline: community vs. clinical-based samples. *Exp Gerontol*. (2021) 145:111216. doi: 10.1016/j.exger.2020.111216

34. Selnes P, Aarsland D, Bjornerud A, Gjerstad L, Wallin A, Hessen E, et al. Diffusion tensor imaging surpasses cerebrospinal fluid as predictor of cognitive decline and medial temporal lobe atrophy in subjective cognitive impairment and mild cognitive impairment. *J Alzheimers Dis*. (2013) 33:723–36. doi: 10.3233/JAD-2012-121603

35. Chen Y, Wang Y, Song Z, Fan Y, Gao T, Tang X. Abnormal white matter changes in Alzheimer's disease based on diffusion tensor imaging: a systematic review. *Ageing Res Rev*. (2023) 87:101911. doi: 10.1016/j.arr.2023.101911

36. Chao YP, Liu PB, Wang PN, Cheng CH. Reduced inter-voxel white matter integrity in subjective cognitive decline: diffusion tensor imaging with tract-based spatial statistics analysis. *Front Aging Neurosci*. (2022) 14:810998. doi: 10.3389/fnagi.2022.810998

37. Wang S, Rao J, Yue Y, Xue C, Hu G, Qi W, et al. Altered frequency-dependent brain activation and white matter integrity associated with cognition in characterizing preclinical Alzheimer's disease stages. *Front Hum Neurosci*. (2021) 15:625232. doi: 10.3389/fnhum.2021.625232

38. Taylor JR, Williams N, Cusack R, Auer T, Shafto MA, Dixon M, et al. The Cambridge Centre for Ageing and Neuroscience (Cam-CAN) data repository: structural and functional MRI, MEG, and cognitive data from a cross-sectional adult lifespan sample. *NeuroImage*. (2017) 144:262–9. doi: 10.1016/j.neuroimage.2015.09.018

39. Shafto MA, Tyler LK, Dixon M, Taylor JR, Rowe JB, Cusack R, et al. The Cambridge Centre for Ageing and Neuroscience (Cam-CAN) study protocol: a cross-sectional, lifespan, multidisciplinary examination of healthy cognitive ageing. *BMC Neurol*. (2014) 14:1–25. doi: 10.1186/s12883-014-0204-1

40. Schweizer S, Kievit RA, Emery T, Cam CAN, Henson RN. Symptoms of depression in a large healthy population cohort are related to subjective memory complaints and memory performance in negative contexts. *Psychol Med*. (2018) 48:104–14. doi: 10.1017/S0033291717001519

41. Schilling KG, Archer D, Yeh FC, Rheault F, Cai LY, Hansen C, et al. Aging and white matter microstructure and macrostructure: a longitudinal multi-site diffusion MRI study of 1218 participants. *Brain Struct Funct*. (2022) 227:2111–25. doi: 10.1007/s00429-022-02503-z

42. Ohlhauser L, Parker AF, Smart CM, Gawryluk JR. Alzheimer's disease Neuroimaging I. White matter and its relationship with cognition in subjective cognitive decline. *Alzheimers Dement*. (2019) 11:28–35. doi: 10.1016/j.dadm.2018.10.008

43. Catani M, Howard RJ, Pajevic S, Jones DK. Virtual in vivo interactive dissection of white matter fasciculi in the human brain. *NeuroImage*. (2002) 17:77–94. doi: 10.1006/nimg.2002.1136

44. Folstein MF, Folstein SE, McHugh PR. "Mini-mental state": a practical method for grading the cognitive state of patients for the clinician. *J Psychiatr Res*. (1975) 12:189–98. doi: 10.1016/0022-3956(75)90026-6

45. Wechsler D. *Wechsler memory scale third UK E*. London: Harcourt Assessment (1999).

46. Veraart J, Novikov DS, Christiaens D, Ades-Aron B, Sijbers J, Fieremans E. Denoising of diffusion MRI using random matrix theory. *NeuroImage*. (2016) 142:394–406. doi: 10.1016/j.neuroimage.2016.08.016

47. Veraart J, Fieremans E, Novikov DS. Diffusion MRI noise mapping using random matrix theory. *Magn Reson Med*. (2016) 76:1582–93. doi: 10.1002/mrm.26059

48. Cordero-Grande L, Christiaens D, Hutter J, Price AN, Hajnal JV. Complex diffusion-weighted image estimation via matrix recovery under general noise models. *NeuroImage*. (2019) 200:391–404. doi: 10.1016/j.neuroimage.2019.06.039

49. Kellner E, Dhital B, Kiselev VG, Reisert M. Gibbs-ringing artifact removal based on local subvoxel-shifts. *Magn Reson Med*. (2016) 76:1574–81. doi: 10.1002/mrm.26054

50. Bautista T, O'Muircheartaigh J, Hajnal JV, Tournier J-D, (Ed.) Removal of Gibbs ringing artefacts for 3D acquisitions using subvoxel shifts. *Proc Int Soc Magn Reson Med*; (2021)

51. Andersson JLR, Sotiropoulos SN. An integrated approach to correction for off-resonance effects and subject movement in diffusion MR imaging. *NeuroImage*. (2016) 125:1063–78. doi: 10.1016/j.neuroimage.2015.10.019

52. Jenkinson M, Beckmann CF, Behrens TE, Woolrich MW, Smith SM. FSL. *NeuroImage*. (2012) 62:782–90. doi: 10.1016/j.neuroimage.2011.09.015

53. Smith SM, Jenkinson M, Johansen-Berg H, Rueckert D, Nichols TE, Mackay CE, et al. Tract-based spatial statistics: voxelwise analysis of multi-subject diffusion data. *NeuroImage*. (2006) 31:1487–505. doi: 10.1016/j.neuroimage.2006.02.024

54. Mori S, Wakana S, Van Zijl PC, Nagae-Poetscher L. *MRI atlas of human white matter* Elsevier (2005).

55. Billot B, Greve DN, Puonti O, Thielscher A, Van Leemput K, Fischl B, et al. SynthSeg: segmentation of brain MRI scans of any contrast and resolution without retraining. *Med Image Anal*. (2023) 86:102789. doi: 10.1016/j.media.2023.102789

56. Tukey JW. *Exploratory data analysis* Addison-Wesley Publishing Company (1977).

57. Smith SM, Nichols TE. Threshold-free cluster enhancement: addressing problems of smoothing, threshold dependence and localisation in cluster inference. *NeuroImage*. (2009) 44:83–98. doi: 10.1016/j.neuroimage.2008.03.061

58. Winkler AM, Ridgway GR, Webster MA, Smith SM, Nichols TE. Permutation inference for the general linear model. *NeuroImage*. (2014) 92:381–97. doi: 10.1016/j.neuroimage.2014.01.060

59. Corrada MM, Brookmeyer R, Paganini-Hill A, Berlau D, Kawas CH. Dementia incidence continues to increase with age in the oldest old: the 90+ study. *Ann Neurol*. (2010) 67:114–21. doi: 10.1002/ana.21915

60. Sun SW, Liang HF, Trinkaus K, Cross AH, Armstrong RC, Song SK. Noninvasive detection of cuprizone induced axonal damage and demyelination in the mouse corpus callosum. *Magn Reson Med*. (2006) 55:302–8. doi: 10.1002/mrm.20774

61. Klistorner S, Barnett MH, Wassertha J, Yiannikas C, Barton J, Parratt J, et al. Differentiating axonal loss and demyelination in chronic MS lesions: a novel approach using single streamline diffusivity analysis. *PLoS One*. (2021) 16:e0244766. doi: 10.1371/journal.pone.0244766

62. Klawiter EC, Schmidt RE, Trinkaus K, Liang HF, Budde MD, Naismith RT, et al. Radial diffusivity predicts demyelination in ex vivo multiple sclerosis spinal cords. *NeuroImage*. (2011) 55:1454–60. doi: 10.1016/j.neuroimage.2011.01.007

63. Budde MD, Xie M, Cross AH, Song SK. Axial diffusivity is the primary correlate of axonal injury in the experimental autoimmune encephalomyelitis spinal cord: a quantitative pixelwise analysis. *J Neurosci*. (2009) 29:2805–13. doi: 10.1523/JNEUROSCI.4605-08.2009

64. Xie M, Tobin JE, Budde MD, Chen C-I, Trinkaus K, Cross AH, et al. Rostrocaudal analysis of Corpus callosum demyelination and axon damage across disease stages refines diffusion tensor imaging correlations with pathological features. *J Neuropathol Exp Neurol*. (2010) 69:704–16. doi: 10.1097/NEN.0b013e3181e3de90

65. Kimura-Ohba S, Yang Y, Thompson J, Kimura T, Salayandia VM, Cosse M, et al. Transient increase of fractional anisotropy in reversible vasogenic edema. *J Cereb Blood Flow Metab*. (2016) 36:1731–43. doi: 10.1177/0271678X16630556

66. Chiang CW, Wang Y, Sun P, Lin TH, Trinkaus K, Cross AH, et al. Quantifying white matter tract diffusion parameters in the presence of increased extra-fiber cellularity and vasogenic edema. *NeuroImage*. (2014) 101:310–9. doi: 10.1016/j.neuroimage.2014.06.064

67. Dhaya I, Griton M, Raffard G, Amri M, Hiba B, Konsman JP. Bacterial lipopolysaccharide-induced systemic inflammation alters perfusion of white matter-rich regions without altering flow in brain-irrigating arteries: relationship to blood-brain barrier breakdown? *J Neuroimmunol*. (2018) 314:67–80. doi: 10.1016/j.jneuroim.2017.11.009

68. Griton M, Dhaya I, Nicolas R, Raffard G, Periot O, Hiba B, et al. Experimental sepsis-associated encephalopathy is accompanied by altered cerebral blood perfusion and water diffusion and related to changes in cyclooxygenase-2 expression and glial cell morphology but not to blood-brain barrier breakdown. *Brain Behav Immun*. (2020) 83:200–13. doi: 10.1016/j.bbi.2019.10.012

69. Dong JW, Jelescu IO, Ades-Aron B, Novikov DS, Friedman K, Babb JS, et al. Diffusion MRI biomarkers of white matter microstructure vary nonmonotonically with increasing cerebral amyloid deposition. *Neurobiol Aging*. (2020) 89:118–28. doi: 10.1016/j.neurobiolaging.2020.01.009

70. Wolf D, Fischer FU, Scheurich A, Fellgiebel A. Alzheimer's Disease Neuroimaging I. Non-linear association between cerebral amyloid deposition and white matter

71. Fick RHJ, Daianu M, Pizzolato M, Wassermann D, Jacobs RE, Thompson PM, et al. Comparison of biomarkers in transgenic Alzheimer rats using multi-Shell diffusion MRI. *Computational Diffusion MRI Math Visualiz*. (2017). 187–199

72. Viviano RP, Hayes JM, Pruitt PJ, Fernandez ZJ, van Rooden S, van der Grond J, et al. Aberrant memory system connectivity and working memory performance in subjective cognitive decline. *NeuroImage*. (2019) 185:556–64. doi: 10.1016/j.neuroimage.2018.10.015

73. Wei Y-C, Hsu C-CH, Huang W-Y, Chen Y-L, Lin C, Chen C-K, et al. White matter integrity underlies the physical-cognitive correlations in subjective cognitive decline. *Front Aging Neuroscience*. (2021) 13:700764. doi: 10.3389/fnagi.2021.700764

74. McKinnon ET, Jensen JH. Measuring intra-axonal T2 in white matter with direction-averaged diffusion MRI. *Magn Reson Med*. (2019) 81:2985–94. doi: 10.1002/mrm.27617

75. Luo C, Li M, Qin R, Chen H, Yang D, Huang L, et al. White matter microstructural damage as an early sign of subjective cognitive decline. *Front Aging Neurosci*. (2020) 11:378. doi: 10.3389/fnagi.2019.00378

76. Stenset V, Bjornerud A, Fjell AM, Walhovd KB, Hofoss D, Due-Tonnessen P, et al. Cingulum fiber diffusivity and CSF T-tau in patients with subjective and mild cognitive impairment. *Neurobiol Aging*. (2011) 32:581–9. doi: 10.1016/j.neurobiolaging.2009.04.014

77. Archer DB, Moore EE, Pamidimukkala U, Shashikumar N, Pechman KR, Blennow K, et al. The relationship between white matter microstructure and self-perceived cognitive decline. *NeuroImage Clin*. (2021) 32:102794. doi: 10.1016/j.nicl.2021.102794

78. Shao W, Li X, Zhang J, Yang C, Tao W, Zhang S, et al. White matter integrity disruption in the pre-dementia stages of Alzheimer's disease: from subjective memory impairment to amnestic mild cognitive impairment. *Eur J Neurol*. (2019) 26:800–7. doi: 10.1111/ene.13892

79. Li X-Y, Tang Z-C, Sun Y, Tian J, Liu Z-Y, Han Y. White matter degeneration in subjective cognitive decline: a diffusion tensor imaging study. *Oncotarget*. (2016) 7:54405–14. doi: 10.18632/oncotarget.10091

80. Selnes P, Fjell AM, Gjerstad L, Bjørnerud A, Wallin A, Due-Tønnessen P, et al. White matter imaging changes in subjective and mild cognitive impairment. *Alzheimers Dement*. (2012) 8:S112–21. doi: 10.1016/j.jalz.2011.07.001

81. Wen Q, Mustafi SM, Li J, Risacher SL, Tallman E, Brown SA, et al. White matter alterations in early-stage Alzheimer's disease: a tract-specific study. *Alzheimers Dement*. (2019) 11:576–87. doi: 10.1016/j.dadm.2019.06.003

82. Motovylyak A, Vogt NM, Adluru N, Ma Y, Wang R, Oh JM, et al. Age-related differences in white matter microstructure measured by advanced diffusion MRI in healthy older adults at risk for Alzheimer's disease. *Aging Brain*. (2022) 2:100030. doi: 10.1016/j.nbas.2022.100030

83. Jelescu IO, Zurek M, Winters KV, Veraart J, Rajaratnam A, Kim NS, et al. In vivo quantification of demyelination and recovery using compartment-specific diffusion MRI metrics validated by electron microscopy. *NeuroImage*. (2016) 132:104–14. doi: 10.1016/j.neuroimage.2016.02.004

84. Moody JF, Dean DC, Kecskemeti SR, Blennow K, Zetterberg H, Kollmorgen G, et al. Associations between diffusion MRI microstructure and cerebrospinal fluid markers of Alzheimer's disease pathology and neurodegeneration along the Alzheimer's disease continuum. *Alzheimers Dement*. (2022) 14:e12381. doi: 10.1002/dad2.12381

85. Roe JM, Vidal-Pineiro D, Sorensen O, Brandmaier AM, Duzel S, Gonzalez HA, et al. Asymmetric thinning of the cerebral cortex across the adult lifespan is accelerated in Alzheimer's disease. *Nat Commun*. (2021) 12:721. doi: 10.1038/s41467-021-21057-y

86. Chad JA, Pasternak O, Salat DH, Chen JJ. Re-examining age-related differences in white matter microstructure with free-water corrected diffusion tensor imaging. *Neurobiol Aging*. (2018) 71:161–70. doi: 10.1016/j.neurobiolaging.2018.07.018

87. O'Donnell LJ, Westin CF. An introduction to diffusion tensor image analysis. *Neurosurg Clin N Am*. (2011) 22:185–96. doi: 10.1016/j.nec.2010.12.004

88. Alexander AL, Lee JE, Lazar M, Field AS. Diffusion tensor imaging of the brain. *Neurotherapeutics J Am Soc Exp NeuroTherap*. (2007) 4:316–29. doi: 10.1016/j.nurt.2007.05.011

89. Promteangtrong C, Kolber M, Ramchandra P, Moghbel M, Houshmand S, Scholl M, et al. Multimodality imaging approach in Alzheimer disease. Part I: structural MRI, functional MRI, diffusion tensor imaging and magnetization transfer imaging. *Dement Neuropsychol*. (2015) 9:318–29. doi: 10.1590/1980-57642015DN94000318